

Time-dependent AMS-02 electron-positron fluxes in an *extended* force-field model

Marco Kuhlen and Philipp Mertsch

*Institute for Theoretical Particle Physics and Cosmology (TTK),
RWTH Aachen University, 52056 Aachen, Germany*

The magnetised solar wind modulates the galactic cosmic ray flux in the heliosphere up to rigidities as high as 40 GeV. In this work, we present a new and straightforward extension of the force-field model that takes into account charge-sign dependent modulation due to drifts in the heliospheric magnetic field. We have validated our semi-analytical approach via comparison to a fully numerical code. Our model nicely reproduces the AMS-02 measurements and we find the strength of diffusion and drifts to be strongly correlated with the heliospheric tilt angle and magnitude of the magnetic field. We are able to predict the electron and positron fluxes beyond the range for which measurements by AMS-02 have been presented. We have made an example script for the semi-analytical model publicly available.

Introduction.—Upon entering the heliosphere, Galactic cosmic rays encounter the magnetised solar wind and are thus subject to a number of transport processes: advection with the wind, diffusion in the small-scale turbulent magnetic field, drifts due to variations of the large-scale field and adiabatic energy losses in the expanding flow. Together, these effects suppress the fluxes of cosmic rays at Earth compared to the interstellar fluxes. Collectively this process is referred to as solar modulation. (See Ref. [1] for a review.) It is lore that solar modulation is negligible above rigidities of ~ 10 GV, but with the small statistical and systematic errors of modern experiments this number is likely higher. AMS-02, for instance, has reported time variations of the proton and Helium fluxes which must be attributed to solar activity up to rigidities of 40 GV [2].

For the modelling of solar modulation, two approaches have been adopted in the literature: Numerical codes solve the transport equation for models of the heliosphere of varying sophistication [3–6] and have been successfully applied to time-dependent data, too (e.g. [7–9]). While such approaches have the potential to reproduce observations elsewhere in the heliosphere and thus provide a more global picture, the complexity comes at the price of a large number of in principle unknown parameters. These parameters need to be determined by fitting the models to various observables. However, as the input interstellar fluxes depend also on unknown parameters, running such global fits is prohibitively expensive.

Phenomenological studies of Galactic cosmic ray transport on the other hand oftentimes employ the classic force-field model of Gleeson and Axford [10]. This model is conceptually simple and all the complexity of the heliosphere is condensed into only one parameter, the Fisk potential, which can be easily determined by fitting to data. In addition, allowing for this electro-static potential to be time-dependent, some degree of correlation between solar activity and this parameter can be found. On the downside, the force-field model assumes a higher degree of symmetry and ignores transport processes that must be important, in particular drifts. Most impor-

tantly, the force-field model has trouble reproducing the measured fluxes. One example is crossing of fluxes, e.g. the proton fluxes measured by AMS-02 during Bartels rotations 2460 and 2476 cross at 4 GeV [11]. In the force-field model, fluxes modulated with different potentials differ at all energies and never cross.

A number of authors have tried to allow for more freedom while maintaining the simplicity of the force-field model, for instance by making the force-field potential rigidity-dependent [12, 13]. Here, we follow a different approach and present a systematic extension of the conventional force-field model. We start from the general transport equation in 2D that includes drifts and then reduce it—under a limited number of assumptions—to a force-field like structure. Our semi-analytical model allows calculating the modulated fluxes at a very moderate computational cost. Our model contains two free parameters per time interval which we determine by fitting to the AMS-02 data. We further investigate temporal correlations with solar wind parameters and replace the free parameters by a linear model of tilt angle and magnetic field strength. Combining the semi-analytical model with the solar wind correlations allows reproducing the AMS-02 data and predicting electron and positron fluxes beyond the range of measurements by AMS-02. We have made an example script for the semi-analytical model available in both Python and C++ [20].

Semi-analytical model—The propagation of cosmic rays in the heliosphere is generally described in terms of a transport equation,

$$\frac{\partial f}{\partial t} + \nabla \cdot (C \mathbf{V} f - K \cdot \nabla f) + \frac{1}{3p^2} \frac{\partial}{\partial p} (p^3 \mathbf{V} \cdot \nabla f) = q, \quad (1)$$

where f is the cosmic ray phase space density with momenta p measured in the observer frame, $C = -(\partial f / \partial p) / 3$ is the Compton-Getting factor [14], \mathbf{V} denotes the solar wind velocity, K is the diffusion tensor, the third term on the left hand side describes the adiabatic losses in the expanding solar wind and q is a source term.

We assume a steady state and follow the conventional

force-field approach insofar as we ignore the adiabatic energy losses in the fixed frame [15]. In the absence of sources the streaming ($\mathbf{C}\mathbf{V}f - \mathbf{K} \cdot \nabla f$) is thus divergence-free and its integral over an arbitrary surface must vanish. After some manipulations [21] this leads to a partial differential equation for $\tilde{f} = \tilde{f}(r, p)$

$$\frac{\partial \tilde{f}}{\partial r} + \frac{p\tilde{V}}{3\tilde{K}_{rr}} \frac{\partial \tilde{f}}{\partial p} = \frac{\tilde{v}_{gc,r}}{\tilde{K}_{rr}} \tilde{f}, \quad (2)$$

where tildes denote (weighted) polar angle averages and $\tilde{v}_{gc,r}$ is the average of the gradient curvature drift. The boundary condition is $\tilde{f}(r_{\max}, p) = f_{\text{LIS}}(p)$, r_{\max} being the radius of the heliosphere. Note that absorbing the non-trivial polar angle dependencies into the averaged quantities has significantly reduced the complexity.

We can solve eq. (2) using the method of characteristics,

$$\tilde{f}(r, p) = f_{\text{LIS}}(p_{\text{LIS}}(r, p)) e^{-\int_0^r dr' \frac{\tilde{v}_{gc,r}(r', p_{\text{LIS}}(r', p))}{\tilde{K}_{rr}(r', p_{\text{LIS}}(r', p))}}, \quad (3)$$

where we have defined $p_{\text{LIS}}(r', p') = p_{r', p'}(r_{\max})$ with $p_{r', p'}(r)$ a solution of the initial value problem

$$\frac{dp}{dr} = \frac{p\tilde{V}}{3\tilde{K}_{rr}}, \quad (4)$$

with $p(r') = p'$.

We will model only the momentum dependence of \tilde{K}_{rr} , $\tilde{v}_{gc,r}$ and \tilde{V} and absorb their normalisation as well as the effect of possible spatial dependencies into scaling factors by making the following replacements in eqs. (3) and (4):

$$\frac{\tilde{v}_{gc,r}}{\tilde{K}_{rr}} \rightarrow g_2 \frac{\tilde{v}_{gc,r}}{\tilde{K}_{rr}} \quad \text{and} \quad \frac{p\tilde{V}}{3\tilde{K}_{rr}} \rightarrow g_1 \frac{p\tilde{V}}{3\tilde{K}_{rr}}. \quad (5)$$

The scaling factors g_1 and g_2 will be determined by fitting to data.

Validation—In order to verify the validity of the approximations made in deriving eqs. (3) and (4), we have solved the transport eq. (1) directly using our own finite-difference code. For the numerical solution, we need to specify a particular heliospheric transport model. The model adopted is closely emulating one that has been successfully applied to data from the PAMELA experiment [7] with some simplifications [22]. Using the numerical code, we have confirmed that the adiabatic term, i.e. the last term on the left-hand-side of eq. (1), always contributes less than 10% to the transport equation [23].

For the semi-analytical model, we adopt fiducial parametrisations for the rigidity-dependencies of \tilde{K}_{rr} , $\tilde{v}_{gc,r}$ and \tilde{V} that follow the rigidity-dependencies used in the numerical code. The diffusion coefficient is modelled as a softly broken power law in rigidity R (understood to be measured in GV),

$$\tilde{K}_{rr} = K_0 R^a \left(\frac{R^c + R_k^c}{1 + R_k^c} \right)^{(b-a)/c}, \quad (6)$$

with a normalization $K_0 = 30 \text{ AU}^2/\text{d}$, power law indices $a = 0$ and $b = 1.55$, $c = 3.5$ and a break rigidity $R_k = 0.28$ fixed to values obtained in previous studies [7]. The radial drift velocity is parametrised as

$$\tilde{v}_{gc,r} = \kappa_0 \frac{R}{3B_0} \frac{10R^2}{1 + 10R^2}, \quad (7)$$

where we set $\kappa_0 = 1 \text{ AU}/\text{d}$ and the magnetic field B_0 is measured in μG .

The averaged radial solar wind obtains a momentum dependence due to the non-uniform spatial distribution of cosmic rays in the heliosphere which depends on the polarity cycle. Motivated by results of our numerical simulation it will be modeled as a step function in momentum

$$\tilde{V} = V_0(1 + \Delta V \theta(R - R_b)). \quad (8)$$

While the rigidity R_b and the height of the step ΔV have to be fitted to data for different products of charge sign and magnetic field polarity, the normalization V_0 is degenerate with K_0 and κ_0 and has thus been fixed to 620 km s^{-1} . We note that the momentum dependence of \tilde{V} only affects energies lower than those of the AMS-02 or PAMELA electron and positron measurements.

We have validated our semi-analytical method by confirming that the fluxes modulated according to eqs. (3) and (4) agree with the results from the fully numerical code. Our semi-analytical method always agrees with the code to within 10% which is far better than for the conventional force-field model [24].

Application to experimental data.—In a first step, we determine for each time bin separately the scaling parameters g_1 and g_2 . The resulting modulated fluxes for one exemplary Bartels rotation is shown in Fig. 1 and compared to AMS-02 [16] data. We also show the results from the conventional force-field model. In particular for the case of electrons the agreement with data is much better for the semi-analytical model than for the conventional force field model. One possible reason for remaining deviations of the experimental data from the model are events of heliospheric origin, like coronal mass ejections, which are not taken into account in our model. Other reasons include inaccuracies in the interstellar fluxes adopted or too restrictive rigidity-dependencies of \tilde{K}_{rr} and $\tilde{v}_{gc,r}$.

Prediction of electron-positron fluxes.—While the semi-analytical model with fitted parameters g_1 and g_2 for most time intervals nicely reproduces the data, this procedure is not predictive. In order to *predict* modulated fluxes, we need to model the parameters g_1 and g_2 as a function of time. Physically, we would expect them to be (anti-)correlated with solar wind parameters. For example, g_1 is related to K_0 , which parametrises the strength of diffusion, and could be correlated with a proxy for solar activity, e.g. the tilt angle α , while g_2 , which parametrises the relative strength of drifts, could

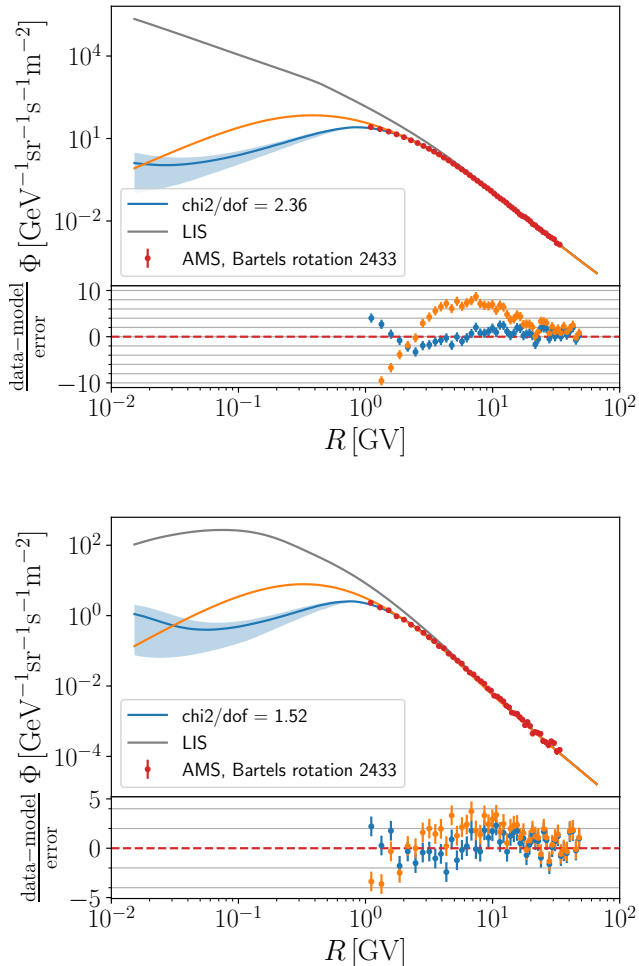


FIG. 1: Fit of our semi-analytical model (blue line) to AMS-02 data [16] and the conventional force-field fit (orange line) for Bartels rotation 2433 for electrons (upper panel) and positrons (lower panel). In both cases the local interstellar spectrum (grey line) is taken from Ref. [17]. The lower part of the plots shows the pull distribution for the fit. For the blue line the step in the solar wind is fitted while for the blue band it is varied between $\Delta V = 0$ and 0.4 .

be anti-correlated with the strength of the magnetic field, B . We stress that both the tilt angle as measured in the solar corona and the field strength as measured by ACE are relatively local observables whereas the cosmic ray particles spend a finite time in the heliosphere. We would therefore expect the fitted parameters to be affected only with a certain delay and after averaging over time.

We have therefore searched for linear correlations between the g_1 and g_2 fitted to AMS-02 data and the tilt angle and magnetic field strength using a moving average of width τ , $\langle \alpha \rangle_\tau$ and $\langle B \rangle_\tau$. It is generally accepted that particles of different signs (q) arrive preferably along different directions in different polarity (A) cycles, specifically for $qA > 0$ ($qA < 0$) particles arrive mostly from

the polar (equatorial) direction. Due to the waviness of the current sheet propagation through the equatorial region takes longer than through the polar region and this implies also different delays for $qA > 0$ and $qA < 0$ with electrons ($q < 0$) in an $A > 0$ cycle experiencing a similar, large delay as positrons ($q > 0$) in an $A < 0$ cycle. We therefore allow for different widths τ for different qA .

We find good correlations (Pearson correlation coefficients of ~ 0.9) between g_1 and $\langle \alpha \rangle_\tau$ for widths of $\tau = 12$ and 39 Bartels rotations for $qA > 0$ and $qA < 0$, respectively. For g_2 , we find an anti-correlation (~ -0.65) with $\langle B \rangle_\tau$ for widths of ~ 5 Bartels rotations. We therefore model the scaling factors as $g_1^\pm = a_1^\pm + b_1^\pm \langle \alpha \rangle_\tau$ and $g_2^\pm = a_2^\pm + b_2^\pm \langle B \rangle_\tau$. To allow for a smoother transition around the solar maximum we adopt τ 's of 21 and 30 Bartels rotations for $qA > 0$ and $qA < 0$ closer to the solar maximum. We summarise the time ranges and averaging widths adopted in Tbl. I. The beginning and end of the ranges correspond to regions where the polarity could be determined including an additional delay.

In Fig. 2, we show the electron fluxes and positron-to-electron ratios as a function of time for different energy ranges. While our model nicely reproduces the measurements by AMS-02, we can predict the fluxes and the ratio also at other times. First, our model can be straightforwardly extended to earlier times. We note that we also reproduce the measurements of PAMELA even though PAMELA data have not been used in the fitting of the coefficients a_1^\pm , b_1^\pm , a_2^\pm or b_2^\pm . Second, we can also make a prediction for the fluxes and the ratio for the range for which measurements of α and B are available, in principle until the end of the $A > 0$ polarity cycle. As a general trend, we would expect the tilt angle to start rising again soon, leading to a falling positron ratio and subsequent maxima in the positron and electron fluxes.

Conclusion.—We have presented a 2D semi-analytical model that incorporates charge-sign dependent modulation effects due to gradient curvature drifts in the solar magnetic field. We have validated our model by comparing to the results of our finite-difference code and found that the semi-analytical model is significantly more accurate than the conventional force field model. Our model has four free parameters, two of which encode the strength of diffusion and drifts.

It is remarkable that allowing these two free param-

start	end	τ_-	τ_+	a_1^-	a_1^+	b_1^-	b_1^+	a_2^-	a_2^+	b_2^-	b_2^+
[BR]						[1/deg]				[1/ μ G]	
2239	2435	12	39	1.79	-0.32	0.025	0.082	1.50	5.80	-0.441	-1.30
2435	2460	21	30	-2.77	-0.88	0.121	0.071	7.59	7.34	-1.62	-1.57
2460	2485	30	21	5.14	-0.46	0.012	0.068	6.18	5.46	-1.31	-1.16
2485	2530	39	12	0.37	-1.57	0.094	0.107	-0.049	3.95	-0.313	-0.808

TABLE I: Interval ranges and averaging widths for electrons (τ_-) and positrons (τ_+) as well as model coefficients.

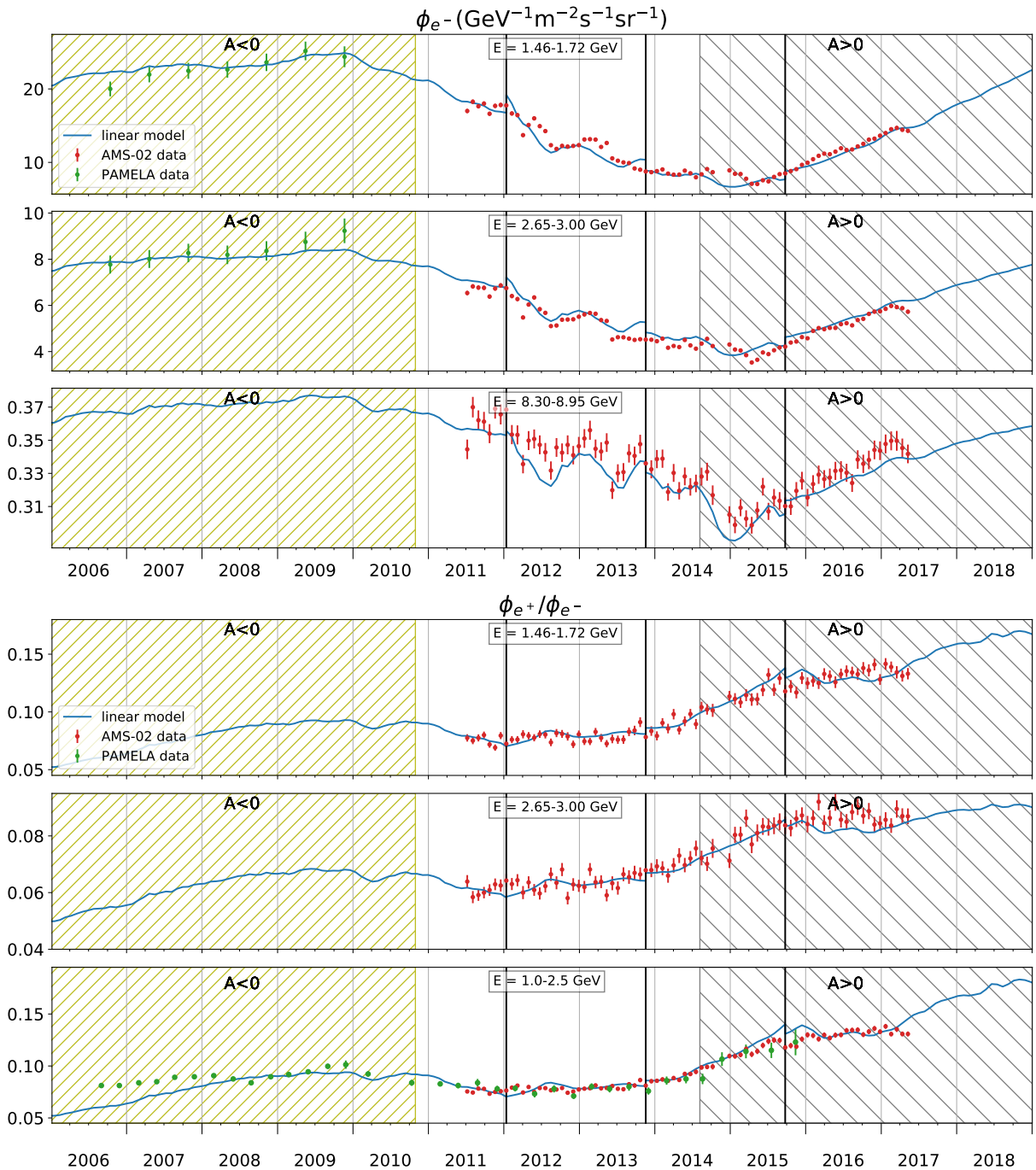


FIG. 2: Time-dependent electron flux (upper panels) and positron ratio (lower panels), calculated with our linear model (blue line) and compared to AMS-02 data (red dots). The bottom panel shows an average over multiple bins in order to compare to PAMELA data [18] (green dots) with wider energy bins. The vertical lines show the transitions between different ranges around the solar maximum. The hatched regions before 2011 and starting in 2014 denote the periods for which the polarity could be unambiguously determined [19].

eters to vary per time interval we can fit the time-dependent AMS-02 electron and positron fluxes rather accurately. Introducing in addition a linear model relating these two parameters to solar wind parameters, we can reproduce not only the AMS-02 measurements, but

also the PAMELA electrons fluxes which do not overlap with the AMS-02 electron fluxes. We can also predict the electron and positron fluxes beyond the range for which data has been published. We stress that our method is significantly faster than fully numerical methods and

more accurate than the standard force field model. It can thus be applied to large datasets with fine time binning like the current AMS-02 data.

Acknowledgments.—We are grateful to Henning Gast, Stefan Schael and Andrea Vittino for helpful discussions.

-
- [1] Marius Potgieter. Solar Modulation of Cosmic Rays. *Living Rev. Solar Phys.*, 10:3, 2013. doi: 10.12942/lrsp-2013-3.
- [2] M. Aguilar, L. Ali Cavazonza, B. Alpat, G. Ambrosi, L. Arruda, N. Attig, S. Aupetit, P. Azzarello, A. Bachlechner, and F. Barao. Observation of Fine Time Structures in the Cosmic Proton and Helium Fluxes with the Alpha Magnetic Spectrometer on the International Space Station. *Phys. Rev. Lett.*, 121(5):051101, Aug 2018. doi: 10.1103/PhysRevLett.121.051101.
- [3] Rolf Kappl. Charge-sign dependent solar modulation for everyone. *J. Phys. Conf. Ser.*, 718(5):052020, 2016. doi: 10.1088/1742-6596/718/5/052020.
- [4] Andrea Vittino, Carmelo Evoli, and Daniele Gaggero. Cosmic-ray transport in the heliosphere with HelioProp. *PoS, ICRC2017:024*, 2018. doi: 10.22323/1.301.0024. [35,24(2017)].
- [5] M. J. Boschini, S. Della Torre, M. Gervasi, G. La Vacca, and P. G. Rancoita. Propagation of cosmic rays in heliosphere: The HELMOD model. *Adv. Space Res.*, 62(10):2859–2879, Nov 2018. doi: 10.1016/j.asr.2017.04.017.
- [6] O. P. M. Aslam, D. Bisschoff, M. S. Potgieter, M. Boezio, and R. Munini. Modeling of Heliospheric Modulation of Cosmic-Ray Positrons in a Very Quiet Heliosphere. *ApJ*, 873(1):70, Mar 2019. doi: 10.3847/1538-4357/ab05e6.
- [7] M. S. Potgieter, E. E. Vos, R. Munini, M. Boezio, and V. Di Felice. Modulation of Galactic Electrons in the Heliosphere during the Unusual Solar Minimum of 2006-2009: A Modeling Approach. *ApJ*, 810:141, September 2015. doi: 10.1088/0004-637X/810/2/141.
- [8] Matteo Jerome Boschini, Stefano Della Torre, Massimo Gervasi, Giuseppe La Vacca, and Pier Giorgio Rancoita. The HelMod Model in the Works for Inner and Outer Heliosphere: from AMS to Voyager Probes Observations. *arXiv e-prints*, art. arXiv:1903.07501, Mar 2019.
- [9] C. Corti, M. S. Potgieter, V. Bindi, C. Consolandi, C. Light, M. Palermo, and A. Popkow. Numerical Modeling of Galactic Cosmic-Ray Proton and Helium Observed by AMS-02 during the Solar Maximum of Solar Cycle 24. *ApJ*, 871:253, February 2019. doi: 10.3847/1538-4357/aafac4.
- [10] L. J. Gleeson and W. I. Axford. Solar Modulation of Galactic Cosmic Rays. *ApJ*, 154:1011, December 1968. doi: 10.1086/149822.
- [11] Alessandro Cuoco, Jan Heisig, Lukas Klamt, Michael Korsmeier, and Michael Krämer. Scrutinizing the evidence for dark matter in cosmic-ray antiprotons. *Phys. Rev.*, D99(10):103014, 2019. doi: 10.1103/PhysRevD.99.103014.
- [12] Ilias Cholis, Dan Hooper, and Tim Linden. A Predictive Analytic Model for the Solar Modulation of Cosmic Rays. *Phys. Rev.*, D93(4):043016, 2016. doi: 10.1103/PhysRevD.93.043016.
- [13] Jan Gieseler, Bernd Heber, and Konstantin Herbst. An empirical modification of the force field approach to describe the modulation of galactic cosmic rays close to Earth in a broad range of rigidities. *J. Geophys. Res. Space Phys.*, 122(11):10,964–10,979, 2017. doi: 10.1002/2017JA024763.
- [14] Arthur H. Compton and Ivan A. Getting. An Apparent Effect of Galactic Rotation on the Intensity of Cosmic Rays. *Physical Review*, 47(11):817–821, Jun 1935. doi: 10.1103/PhysRev.47.817.
- [15] R. A. Caballero-Lopez and H. Moraal. Limitations of the force field equation to describe cosmic ray modulation. *J. Geophys. Res. Space Phys.*, 109(A1):A01101, Jan 2004. doi: 10.1029/2003JA010098.
- [16] M. Aguilar et al. Observation of complex time structures in the cosmic-ray electron and positron fluxes with the alpha magnetic spectrometer on the international space station. *Phys. Rev. Lett.*, 121:051102, Jul 2018. doi: 10.1103/PhysRevLett.121.051102. URL <https://link.aps.org/doi/10.1103/PhysRevLett.121.051102>.
- [17] Andrea Vittino, Philipp Mertsch, Henning Gast, and Stefan Schael. Breaks in interstellar spectra of positrons and electrons derived from time-dependent AMS data. *Phys. Rev.*, D100(4):043007, 2019. doi: 10.1103/PhysRevD.100.043007.
- [18] R. Munini et al. Ten years of positron and electron solar modulation measured by the PAMELA experiment. *PoS, ICRC2017:012*, 2018. doi: 10.22323/1.301.0012.
- [19] M. Krainev, B. Bazilevskaya, M. Kalinin, A. Svirzhevskaya, and N. Svirzhevsky. GCR intensity during the sunspot maximum phase and the inversion of the heliospheric magnetic field. *PoS*, 2015. doi: 10.22323/1.236.0081.
- [20] <https://git.rwth-aachen.de/kuhlenmarco/effmod-code>
- [21] See Supplemental Material for the detailed calculation.
- [22] The details of the heliospheric model are given in the Supplemental Material.
- [23] See the Supplemental Material for a plot.
- [24] Plots for $qA > 0$ and $qA < 0$ are shown in the Supplemental Material.

Time-dependent AMS-02 electron-positron fluxes in an *extended* force-field model: Supplementary Material

Marco Kuhlen and Philipp Mertsch
Institute for Theoretical Particle Physics and Cosmology (TTK),
RWTH Aachen University, 52056 Aachen, Germany

CONVENTIONAL FORCE FIELD MODEL

The conventional force-field model [1, 2] is most easily explained by starting with the cosmic ray transport equation in the form of Gleeson & Webb (cf. e.g. [3]),

$$\frac{\partial f}{\partial t} + \nabla \cdot (C\mathbf{V}f - K \cdot \nabla f) + \frac{1}{3p^2} \frac{\partial}{\partial p} (p^3 \mathbf{V} \cdot \nabla f) = q. \quad (1)$$

Here, f is the cosmic ray phase space density in the fixed frame, $C = -(\partial f / \partial p) / 3$ is the Compton-Getting factor, \mathbf{V} denotes the solar wind, K is the diffusion tensor and the third term on the left hand side describes the adiabatic losses in the expanding solar wind.

Assuming a steady state $\partial f / \partial t = 0$, no sources $q = 0$ and neglecting the adiabatic momentum loss rate in the fixed frame, $\langle \dot{p} \rangle = \frac{1}{3} \mathbf{V} \cdot \nabla f / f = 0$, this reduces to

$$\nabla \cdot (C\mathbf{V}f - \mathbf{K} \cdot \nabla f) = 0. \quad (2)$$

Note that this does not imply that individual particles do not lose energy. $\langle \dot{p} \rangle = \frac{1}{3} \mathbf{V} \cdot \nabla f / f$ is the average rate of momentum change *in the fixed frame* while the mean rate of change of momentum of an individual particle is $\langle \dot{p} \rangle = -\frac{p}{3} \nabla \cdot \mathbf{V}$ [4].

Assuming spherical symmetry, eq. (2) further reduces to

$$CVf - \kappa \frac{\partial f}{\partial r} = 0, \quad (3)$$

where obviously all structure of the heliospheric magnetic field, anisotropic diffusion and any drift terms are lost. Eq. (3) is also called the zero streaming condition and indeed in an approximate one dimensional solution of the full transport equation it was shown that the advective and diffusive flow almost cancel [5].

Substituting the Compton-Getting factor gives the first order partial differential equation,

$$\frac{\partial f}{\partial r} + \frac{Vp}{3\kappa} \frac{\partial f}{\partial p} = 0, \quad (4)$$

which can now be solved using the method of characteristics, that is f is constant along the characteristics,

$$\frac{\partial p}{\partial r} = \frac{Vp}{3\kappa}. \quad (5)$$

If the diffusion coefficient factorises into a radial and a momentum dependence, $\kappa = \beta \kappa_r(r) \kappa_p(p)$, eq. (5) can easily be integrated to

$$\int_{p_{TOA}}^{p_{LIS}} \frac{\beta \kappa_{p'}}{p'} dp' = \int_{r_{TOA}}^{r_{LIS}} \frac{V}{3\kappa_r(r')} dr' \equiv \phi(r), \quad (6)$$

where the indices TOA and LIS denote the top of the atmosphere and the local interstellar spectrum respectively.

When further assuming $\kappa_p \propto p$ and $\beta \approx 1$ for relativistic particles the force-field $\phi(r)$ reduces to the well-known form $\phi = p_{LIS} - p_{TOA}$.

The conservation of the phase-space density f along characteristics, cf. eq. (4), implies (again for relativistic particles) that

$$\frac{J_{TOA}}{p_{TOA}^2} = \frac{J_{LIS}}{p_{LIS}^2}. \quad (7)$$

EXTENDED FORCE FIELD MODEL

We start by assuming a steady state and follow the conventional force-field approach by neglecting the adiabatic energy losses in the fixed frame [6]. Below, we will show that the adiabatic term always contributes less than 10% to the transport equation (cf. Sec. ‘‘Validation’’ and Fig. 1). In the absence of sources the streaming $\mathbf{F} \equiv C\mathbf{V}f - K \cdot \nabla f$ is thus divergence-free and its integral over an arbitrary surface must vanish. We choose this surface to be a sphere of radius r such that the divergence-free streaming condition in spherical coordinates, $\{r, \theta, \phi\}$, reads

$$\int_0^{\pi/2} d\theta \sin \theta \left(CVf - \left(K_{rr} \frac{\partial f}{\partial r} + K_{r\theta} \frac{1}{r} \frac{\partial f}{\partial \theta} \right) \right) = 0. \quad (8)$$

For the last term, we apply integration by parts,

$$\int_0^{\pi/2} d\theta \sin \theta \left(CVf - K_{rr} \frac{\partial f}{\partial r} \right) + \frac{1}{r} \int_0^{\pi/2} d\theta f \frac{\partial}{\partial \theta} (\sin \theta K_{r\theta}) - \frac{1}{r} [\sin \theta K_{r\theta} f]_0^{\pi/2} = 0.$$

Next, we identify the Compton-Getting factor $C = -(\partial \ln f / \partial \ln p) / 3$, the off-diagonal term of the diffusion tensor $K_{r\theta} = -\kappa_A \sin \psi$ (ψ denoting the spiral angle of the magnetic field) and the radial component of the drift velocity $\partial_\theta (\sin \theta K_{r\theta}) / (r \sin \theta) = v_{gc,r}$ leading to

$$\int_0^{\pi/2} d\theta \sin \theta \left(-\frac{pV}{3} \frac{\partial f}{\partial p} - K_{rr} \frac{\partial f}{\partial r} \right) + \int_0^{\pi/2} d\theta \sin \theta v_{gc,r} f + \frac{1}{r} [\sin \theta \kappa_A \sin \psi f]_0^{\pi/2} = 0. \quad (9)$$

We note that under the assumption that $f(\theta = \pi/2) \approx \tilde{f}$, the last term can be absorbed into the previous one (that also contains the drift velocity) if their momentum dependences are identical. This assumption has been verified using the numerical solution of the transport equation. We find good agreement between the third term with $f(\theta = \pi/2)$ and the same term with \tilde{f} in all cases where this term gives a meaningful contribution to this equation.

Introducing the angular averages,

$$\tilde{f} = \int_0^{\pi/2} d\theta \sin \theta f, \quad (10)$$

$$\tilde{V} = \left(\partial_p \tilde{f} \right)^{-1} \int_0^{\pi/2} d\theta \sin \theta V \partial_p f, \quad (11)$$

$$\tilde{K}_{rr} = \left(\partial_r \tilde{f} \right)^{-1} \int_0^{\pi/2} d\theta \sin \theta K_{rr} \partial_r f, \quad (12)$$

$$\tilde{v}_{gc,r} = \left(\tilde{f} \right)^{-1} \int_0^{\pi/2} d\theta \sin \theta v_{gc,r} f, \quad (13)$$

this leads to the partial differential equation

$$\frac{\partial \tilde{f}}{\partial r} + \frac{p\tilde{V}}{3\tilde{K}_{rr}} \frac{\partial \tilde{f}}{\partial p} = \frac{\tilde{v}_{gc,r}}{\tilde{K}_{rr}} \tilde{f}. \quad (14)$$

We can solve eq. (14) using the method of characteristics,

$$\tilde{f}(r, p) = f_{\text{LIS}}(p_{\text{LIS}}(r, p)) e^{-\int_0^r dr' \frac{\tilde{v}_{gc,r}(r', p_{\text{LIS}}(r', p))}{\tilde{K}_{rr}(r', p_{\text{LIS}}(r', p))}}, \quad (15)$$

with the definition $p_{\text{LIS}}(r', p') = p_{r', p'}(r_{\text{max}})$ and where $p_{r', p'}(r)$ is a solution of the initial value problem

$$\frac{dp}{dr} = \frac{p\tilde{V}}{3\tilde{K}_{rr}}, \quad (16)$$

with $p(r') = p'$.

VALIDIATION

In order to verify the validity of the approximations made in deriving eqs. (15) and (16), we have solved the transport eq. (1) directly using our own 2D finite-difference code that is similar in structure to the one by Langer [7]. Below, we specify the particular heliospheric transport model adopted which is closely emulating a model that has been successfully applied to data from the PAMELA experiment [8]. Where necessary, we focus on propagation parameters relevant for relativistic electrons and positrons for application to the recently presented time-dependent measurements of the electron and positron fluxes from AMS-02.

The parametrisation of the radial solar wind is taken as a product of two functions V_r and V_θ that only depend on the radial coordinate and the latitude respectively:

$$\begin{aligned} V_r &= V_0 \left(1 - \exp \left(\frac{40}{3r_0} (r_\odot - r) \right) \right) \\ V_\theta &= 1.5 - 0.5 \cdot \tanh \left(16 \left(\theta - \frac{\pi}{2} + \phi \right) \right), \end{aligned} \quad (17)$$

where $r_0 = 1$ AU is the distance from the Earth to the Sun, $r_\odot = 0.005$ AU is the radius of the Sun, $V_0 = 400$ km s⁻¹ and $\phi = \alpha + 15\pi/180$. Therefore the solar wind varies between ~ 400 km s⁻¹ in the equatorial region and ~ 800 km s⁻¹ in the polar region with the transition depending on the tilt angle α .

In all generality, the diffusion tensor can be written as

$$K = \begin{bmatrix} \kappa_{\parallel} & 0 & 0 \\ 0 & \kappa_{\perp\theta} & \kappa_A \\ 0 & -\kappa_A & \kappa_{\perp r} \end{bmatrix} = K_S + K_A, \quad (18)$$

in a coordinate system with the first coordinate axis aligned with the background magnetic field direction. Here κ_{\parallel} is the diffusion coefficient parallel to the background magnetic field and $\kappa_{\perp\theta}$ and $\kappa_{\perp r}$ are the diffusion coefficients perpendicular to the magnetic field in polar and radial direction, respectively.

Assuming a Parker-like magnetic field the diffusion tensor can be transformed from coordinates aligned with the magnetic field to the corotating frame as

$$\begin{bmatrix} K_{rr} & K_{r\theta} & K_{r\phi} \\ K_{\theta r} & K_{\theta\theta} & K_{\theta\phi} \\ K_{\phi r} & K_{\phi\theta} & K_{\phi\phi} \end{bmatrix} = \begin{bmatrix} \kappa_{\parallel} \cos^2 \psi + \kappa_{\perp r} \sin^2 \psi & -\kappa_A \sin \psi & (\kappa_{\perp r} - \kappa_{\parallel}) \cos \psi \sin \psi \\ \kappa_A \sin \psi & \kappa_{\perp\theta} & \kappa_A \cos \psi \\ (\kappa_{\perp r} - \kappa_{\parallel}) \cos \psi \sin \psi & -\kappa_A \cos \psi & \kappa_{\parallel} \sin^2 \psi + \kappa_{\perp r} \cos^2 \psi \end{bmatrix}, \quad (19)$$

with the ψ the spiral angle of the magnetic field.

The parametrisation of the transport parameters is based on the model described in [8]. The parallel diffusion coefficient is parametrised as a softly broken power law,

$$\kappa_{\parallel} = \kappa_{\parallel}^0 \beta \left(\frac{B_0}{B} \right) (R/R_0)^a \left[\frac{(R/R_0)^c + (R_k/R_0)^c}{1 + (R_k/R_0)^c} \right]^{(b-a)/c} \quad (20)$$

Here, R is the particle rigidity defined as momentum over particle charge and $\beta = v/c$, $B_0 = 1$ nT and $R_0 = 1$ GV are reference values for the magnetic field strength and momentum, R_k is the break rigidity and κ_{\parallel}^0 is a normalisation factor of the order of ~ 30 AU² d⁻¹. For $R/R_k \ll 1$, $\kappa_{\parallel} \propto R^a$, whereas for $R/R_k \gg 1$, $\kappa_{\parallel} \propto R^b$ and the parameter c determines the softness of the break. The parameters of the diffusion coefficient can be determined by fitting the model to experimental data. Throughout this work we set $a = 0$ which is consistent with theoretical calculations of the mean free path of electrons [9]. For simplicity the diffusion coefficients perpendicular to the magnetic field have the same energy dependence and are only rescaled by a factor $f_{\perp} = 0.02$.

The term of the transport equation involving the anti-symmetric part of the diffusion tensor K_A can be rewritten as an additional advection term with the drift velocity

$$\mathbf{V}_d = \nabla \times (\kappa_A \mathbf{e}_B), \quad (21)$$

where \mathbf{e}_B is a unit vector pointing in the direction of the regular magnetic field. Under the assumption of weak scattering the drift coefficient is

$$\kappa_A = \kappa_A^0 \frac{v(R/R_0)}{3cB}, \quad (22)$$

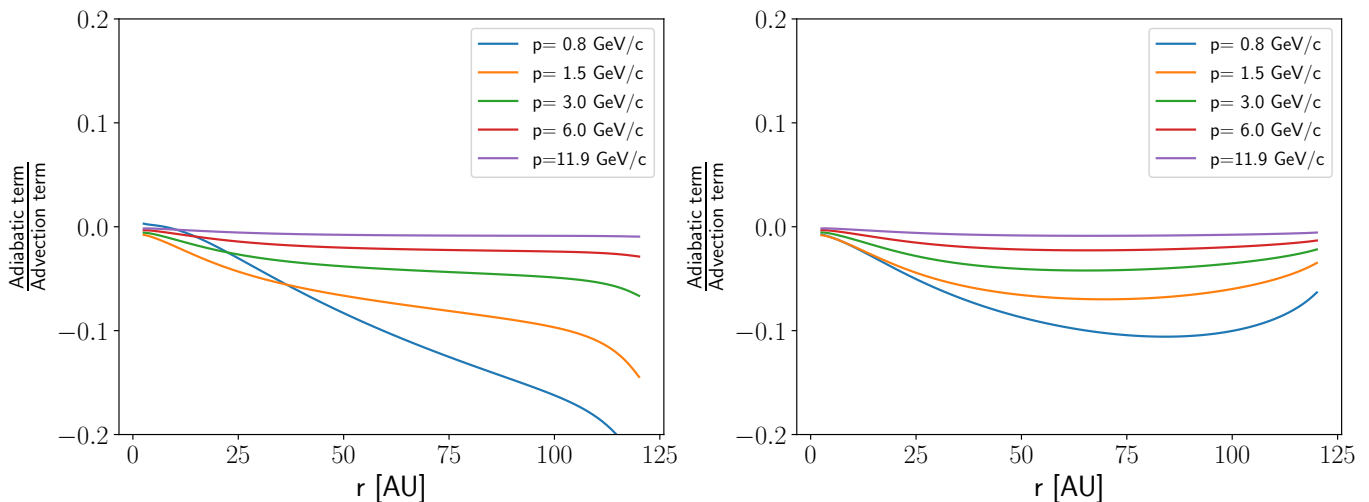


FIG. 1: Ratio of the adiabatic energy loss in eq. (1) to the advection term for different rigidities as a function of radial distance for a tilt angle of $\alpha = 10^\circ$. The adiabatic term contributes less than 10% to the transport equation in the inner heliosphere for intermediate energies. It gets slightly more important for low energies. The left panel is for $qA < 0$ and the right panel for $qA > 0$.

with κ_A^0 a dimensionless constant. The cases $\kappa_A^0 = 1, 0.5$ and 0 have been referred to as refer to as “full drifts”, “half drifts” and “no drifts”, respectively [10].

The weak scattering form of κ_A cannot be used to explain the small latitudinal gradients observed by Ulysses [11], but the modification,

$$\kappa_A = \kappa_A^0 \frac{v(R/R_0)}{3cB} \left(\frac{10(R/R_0)^2}{1 + 10(R/R_0)^2} \right), \quad (23)$$

leads to better agreement with data since it reduces drifts for particles with very low energies slightly [12]. This choice for κ_A is also consistent with numerical simulations done by Giacalone et al. [13].

Given the fully numerical code and the heliospheric model described above, we can check the validity of the assumption made in deriving eq. (15). The most fundamental one is the neglect of the adiabatic term in the transport equation (1). In Fig. 1, we compare the contribution from the adiabatic term, $\partial/\partial p (p^3 \mathbf{V} \cdot \nabla f) / (3p^2)$ to the advective term, $\nabla \cdot (C \mathbf{V} f)$. (The comparison of the adiabatic to the diffusive term $\nabla \cdot (K \cdot \nabla f)$ leads to similar results.) It can be seen that the contribution from the adiabatic term is larger in the outer heliosphere than close to Earth. Furthermore, at rigidities above ~ 1 GV, the adiabatic term generally contributes less than 10% to the transport equation, in particular for $qA > 0$. We thus conclude that the neglect of the adiabatic term is justified.

Next, we check whether the fluxes modulated according to eqs. (15) and (16) agree with the results from the fully numerical code. The transport parameters are as explained in the main part of the letter. In Fig. 2 we show the results of fitting our semi-analytical model (eqs. 15 and 16) to the results from the numerical code. The fit agrees with the numerical solution to within less than 10%. We find significantly better agreement than with the conventional force-field model.

-
- [1] L. J. Gleeson and W. I. Axford. Solar Modulation of Galactic Cosmic Rays. *ApJ*, 154:1011, December 1968. doi: 10.1086/149822.
 - [2] L. J. Gleeson and I. H. Urch. Energy losses and modulation of galactic cosmic rays. *Astrophysics and Space Science*, 11(2):288–308, May 1971. doi: 10.1007/BF00661360.
 - [3] R. A. Caballero-Lopez and H. Moraal. Limitations of the force field equation to describe cosmic ray modulation. *J. Geophys. Res. Space Phys.*, 109(A1):A01101, Jan 2004. doi: 10.1029/2003JA010098.
 - [4] G. M. Webb and L. J. Gleeson. On the equation of transport for cosmic-ray particles in the interplanetary region. *Astrophysics and Space Science*, 60(2):335–351, Feb 1979. ISSN 1572-946X. doi: 10.1007/BF00644337. URL <https://doi.org/10.1007/BF00644337>.

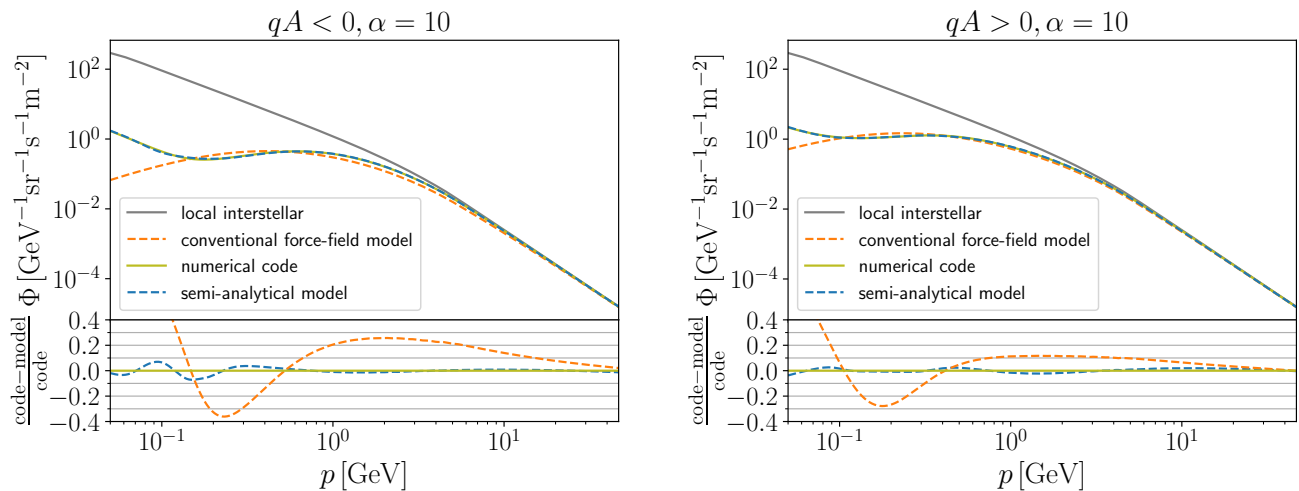


FIG. 2: Fit of our semi-analytical model to the full numerical solution of the transport equation for a tilt angle of $\alpha = 10^\circ$. The left plot shows the fit for $qA < 0$ and the plot on the right $qA > 0$. In the lower panels the relative deviation from the numerical solution is shown.

- [5] L. J. Gleeson and W. I. Axford. The solar radial gradient of galactic cosmic rays. *Canadian Journal of Physics Supplement*, 46:937, 1968. doi: 10.1139/p68-388.
- [6] H. Moraal. Cosmic-Ray Modulation Equations. *Space Sci. Rev.*, 176(1-4):299–319, Jun 2013. doi: 10.1007/s11214-011-9819-3.
- [7] Ulrich Langner. *Effects of Acceleration at the Termination Shock on Cosmic Rays in the Heliosphere*. PhD thesis, Northwest University, Potchefstroom, 2004. PhD thesis.
- [8] M. S. Potgieter, E. E. Vos, R. Munini, M. Boezio, and V. Di Felice. Modulation of Galactic Electrons in the Heliosphere during the Unusual Solar Minimum of 2006–2009: A Modeling Approach. *ApJ*, 810:141, September 2015. doi: 10.1088/0004-637X/810/2/141.
- [9] A. Teufel and R. Schlickeiser. Analytic calculation of the parallel mean free path of heliospheric cosmic rays. I. Dynamical magnetic slab turbulence and random sweeping slab turbulence. *A&A*, 393:703–715, October 2002. doi: 10.1051/0004-6361:20021046.
- [10] R. A. Burger and M. S. Potgieter. The calculation of neutral sheet drift in two-dimensional cosmic-ray modulation models. *ApJ*, 339:501–511, April 1989. doi: 10.1086/167313.
- [11] B. Heber and M.S. Potgieter. Cosmic rays at high heliolatitudes. *Space Sci. Rev.*, 127(117), 2006. URL <https://doi.org/10.1007/s11214-006-9085-y>.
- [12] R. A. Burger, M. S. Potgieter, and B. Heber. Rigidity dependence of cosmic ray proton latitudinal gradients measured by the Ulysses spacecraft: Implications for the diffusion tensor. *J. Geophys. Res.*, 105:27447–27456, December 2000. doi: 10.1029/2000JA000153.
- [13] J. Giacalone and J. R. Jokipii. The Transport of Cosmic Rays across a Turbulent Magnetic Field. *ApJ*, 520:204–214, July 1999. doi: 10.1086/307452.